High-pressure phase of GaP: Structure and chemical ordering

G. Aquilanti,[1,*] H. Libotte,[2] W. A. Crichton,[1] S. Pascarelli,[1] A. Trapananti,[1] and J.-P. Itié[3]
[1]*European Synchrotron Radiation Facility, rue 6 Jules Horowitz, B.P. 220 38043 Grenoble Cedex 09, France*
[2]*Département de Physique, B5, Université de Liège, B4000 Sart-Tilman, Belgium*
[3]*Synchrotron SOLEIL, L'Orme des Merisiers, St Aubin, BP 48, F-91192 Gif-sur-Yvette, France*
(Received 23 April 2007; revised manuscript received 21 June 2007; published 3 August 2007)

The present paper concerns a combined x-ray diffraction and absorption study of gallium phosphide (GaP) at high pressure up to 39 GPa. The aim of this study is twofold: To clarify the nature of the high pressure phase using x-ray diffraction and to determine the degree and the evolution of the short range chemical order using x-ray absorption. The analysis of x-ray diffraction shows that GaP transforms to a *Cmcm* structure and the absence of the "difference reflections" indicates that the *Cmcm* structure lacks long-range chemical order. In this system, the EXAFS is compatible with the hypothesis of a chemically ordered *Cmcm* local environment. The comparison between the XANES region of the spectra and multiple scattering calculations confirms this hypothesis, clearly showing that the *Cmcm* is short-range chemically ordered. The local environment of Ga is given by 6 P atoms and short-range Ga-Ga interactions are not likely to occur in this system, at least up to 39 GPa. This result shows that even in a compound with a relatively low ionicity of the bonds, this parameter dictates the short-range interactions up to very high pressures.

DOI: 10.1103/PhysRevB.76.064103 PACS number(s): 61.10.Nz, 61.10.Ht, 64.70.Kb, 81.05.Ea

I. INTRODUCTION

Angle dispersive x-ray diffraction (ADXRD) applied to high pressure structural studies has led to a reevaluation of the high pressure phase diagram of many materials.[1] At the same time developments in theoretical calculations have allowed to explain the reason of the occurrence of certain high pressure structures and also to predict the occurrence of stable high pressure phases.[2–5] A typical case of this scenario is the reformulation of the structural sequences as a function of pressure of the octect compounds $A^{(n)}B^{(8-n)}$. The unanimously accepted structural sequence for these compounds was the direct transformation from the open fourfold coordinated zincblende (ZB) structure to the quasi-sixfold β-Sn structure, or, first to the sixfold NaCl and then to the β-Sn depending on the ionicity of the bonds.[6] In the light of the systematics, the NaCl structure was found to be stable for a narrow energy range and the β-Sn was found not to occur in any of the III-V and II-VI systems at high pressure and room temperature,[7] although a β-Sn structure has been observed in the more covalent GaSb[8] and in InSb[9] after heating at high pressure. The actual phases were found to have lower symmetry orthorhombic structures with space groups *Cmcm* or *Imm2* and *Imma*. Although the occurrence of the orthorhombic structures has been assessed by ADXRD and their occurrence seems to be systematic for the octet compounds and in particular for the III-V semiconductors,[7] the determination of the site-ordering of the high pressure phases still remains a matter of debate. The determination of the site-ordering of those systems, such as InSb and GaAs, where the two atomic species have very similar scattering power, becomes difficult at high pressures for diffraction techniques, due to important peak broadening. For GaP, where Ga and P have very different scattering powers, ADXRD evidenced a long-range site-disorder at high pressure.[7] However, the fact that the average structure is site-disordered does not exclude the possibility of ordering over a short-range scale.

The local atomic environment yields information on fundamental interactions between atoms. Therefore, only information on local chemical order allows to verify theoretical methods that yield to the formulation of models used to reproduce the thermodynamic and structural properties of matter. In this context, x-ray absorption spectroscopy (XAS) can have an important and complementary role to diffraction techniques because, probing selectively the local environment around the photoabsorber atom, it is able to distinguish chemical order from chemical disorder over a short length scale.

The first structural studies of GaP showed that the high pressure phase had a β-Sn structure.[10,11] A following XAFS study[12] used a model based on the β-Sn structure to fit the experimental data of GaP at high pressure and found that the local environment was well reproduced with such a model, given by 4 P and 2 Ga atoms as first and second neighbors. A more recent experiment using ADXRD has shown that the actual high pressure structure of GaP has a *Cmcm* symmetry with a clear lack of long-range chemical order.[7] A first-principle study of the high pressure structural properties on several III-V compounds[3] has demonstrated that after a first phase transition to an SC16 phase, the latter becomes unstable to the β-Sn structure at 20.3 GPa and to the *Cmcm* at 20.4 GPa. However, as pressure is further increased, the β-Sn structure becomes more stable than *Cmcm*. This overview of previous work suggests conflicting results regarding the nature of the high pressure phase of GaP. In particular, it is worth noting that the structural model based on the β-Sn symmetry, which has been debated, still allowed a good fitting of EXAFS data.[12]

In this contribution, we present an experimental study combining ADXRD and XAS of GaP at high pressure up to 39 GPa. The aim of this work is to elucidate the high pressure phase of GaP and in particular to give an insight on the short-range chemical ordering. The paper is organized as follows. In Sec. II we describe the experimental details of the ADXRD and XAS experiments. In Sec. III we show the data

and their qualitative evolution with pressure. In Sec. IV we present the results deriving from full Rietveld refinement for the ADXRD data and from the EXAFS analysis for the XAS data. In Sec. V we give details of the full multiple scattering calculations of the x-ray absorption near-edge structure (XANES) for the high pressure phase of GaP and we show the comparison with the experimental data. Finally, in Sec. VI we discuss the results and give several conclusions.

II. EXPERIMENT

The XRD and XAS experiments have been both carried out at the European Synchrotron Radiation Facility at beamlines ID30 and ID24 respectively. The pressure was generated using a Le Toullec-type and a Chervin-type diamond anvil cells for the XRD and XAS experiments respectively, equipped with standard diamonds of 320 μm diameter flat. A fine powder of GaP ground from polycrystalline stock (Alfa Aesar, purity 99.999%) was loaded in a stainless steel gasket with a hole of 120 μm of diameter and an initial thickness of 30 μm together with a 4:1 mixture of methanol:ethanol as pressure transmitting medium and a ruby sphere for the pressure measurements.[13] The data were recorded at room temperature. The maximum pressure reached was 39 GPa. For the XRD experiment the wavelength selection was made using a Si (111) monochromator tuned to $\lambda = 0.3738$ Å. Patterns were recorded using a MAR345 image plate detector with 100 μm pixel resolution. The sample-detector distance was calibrated by a Si-filled gasket at the sample position. Two-dimensional image plate data were corrected for spatial distortion and integrated with FiT2D to produce a 2θ-I pattern.[14]

The XAS data were recorded at the gallium *K*-edge ($E = 10.367$ keV). The beam was focussed horizontally by a curved polychromator Si(111) crystal in a Bragg geometry and vertically with a bent Si mirror placed at 2.8 mrad respect to the direct beam.[15] The Bragg diffraction peaks arising from the diamond anvils were removed from the energy range of interest by changing the orientation of the diamond anvil cell and following in real time the intensity of the transmitted beam on a two-dimensional detector. In this case, the Bragg reflections limited the k range of the spectra to ~ 11 Å^{-1}. Although we performed two distinct experiments, the loading conditions (diamonds flats, sample thickness, pressure transmitting medium) were kept the most similar as possible for the two experiments. The only remarkable difference between the two loadings was the position of the ruby sphere that was placed in the center and off-center of the sample for the XRD and XAS experiments respectively. This was necessary for the XAS experiment to avoid any interaction between the x-ray beam and the ruby, detrimental to the data quality.

III. DATA EVOLUTION WITH PRESSURE

Figure 1 shows some ADXRD data at selected pressures. At room pressure GaP crystallizes in a ZB structure. The onset of the phase transition is at 31 GPa with the appearance of new Bragg reflections at $2\theta \sim 9°$ and 12.7°, indicated by arrows in the pattern at 32 GPa of Fig. 1. At 39 GPa the transition is almost complete although the (111) reflection corresponding to the ZB structure at $2\theta \sim 7°$ is still detectable.

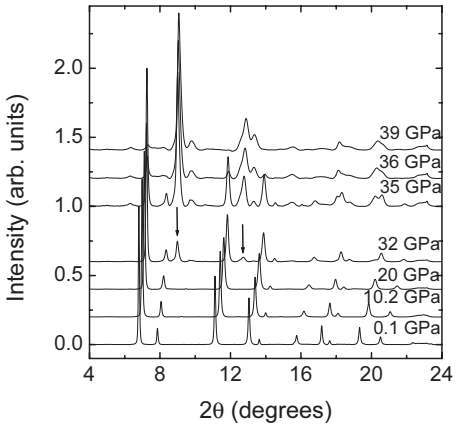

FIG. 1. Background subtracted XRD data at selected pressures. The arrows indicate the new Bragg reflections relative to the high pressure phase of GaP (GaP-II).

Figure 2 shows some XAS data at some selected pressures and the extracted $k\chi(k)$ signals. For this set of data, we observe that the onset of the phase transition is at 26 GPa and at 31 GPa the transition is complete.

The difference in the transition pressure depends on the position of the ruby chip for the pressure measurements. In the XAS data the chip has been placed off center to avoid any interaction between the x-ray beam and the sample resulting in a erroneous normalization of the XAS spectra. As a consequence of this, the pressure is underestimated for the XAS data points. The change in the main frequency of the oscillations from 1.3 GPa to 39 GPa reflects the different local environment around Ga when going from a ZB structure with 4 P first neighbors to a structure with different local symmetry. The data at 28 GPa well describes the mixture of the two phases.

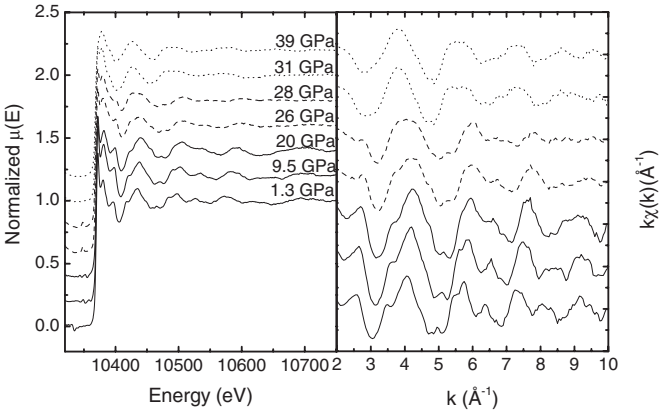

FIG. 2. Left panel: Normalized XAS spectra of GaP at selected pressures. Right panel: Corresponding extracted $k\chi(k)$ EXAFS signals. The spectra drawn in continuous line correspond to the GaP-I, in dashed line to the mixed GaP-I/GaP-II, and in dotted line to the GaP-II.

IV. QUANTITATIVE ANALYSIS

The experimental spectra were analyzed using the Rietveld refinement method.[16] The full-profile refinement was performed using the GSAS[17] package. The background of the spectra was fitted using Chebyshev polynomials of the first kind. The peak profile fitting was based on pseudo-Voigt functions. Moreover, preferred orientation correction was taken into account using the spherical harmonics functions.

The EXAFS data analysis has been performed using the codes from the UWXAFS package.[18] The experimental XAFS functions $\chi(k)$, were obtained after subtracting the embedded-atom absorption background from the measured absorption coefficient and normalizing by the edge step using the program ATHENA.[19] Phase shifts for photoabsorber and backscatterer atoms have been calculated by FEFF8[20] using a self-consistent energy dependent exchange correlation Hedin-Lundqvist potential. Structural data for the GaP phases used by the ATOMS program[21] to prepare the input for FEFF8 were taken from Ref. 22 for the ZB structure, from the Rietveld refinement of ADXRD data for the *Cmcm* structure and from the structural parameters of Itié *et al.*[12] for the β-Sn.

A. GaP-I

The ADXRD data from ambient pressure to 30.2 GPa were Rietveld refined in order to obtain the variation of the cell parameter of GaP in the ZB structure as a function of pressure. Figure 3(a) shows the data and the Rietveld fit of the data at 12.6 GPa. The lattice parameter measured at ambient pressure was 5.455 Å.

The EXAFS data from 0.4 GPa to 23 GPa were also fitted using the structural model based on a ZB structure obtained from diffraction. The k range of the experimental EXAFS function $\chi(k)$ limited the number of structural parameters that could be left free during the minimization procedure. The fits were performed using the theoretical signals relative to single scattering between the photoabsorber and the first three neighbors shells constraining the distances to the crystallographic structure. Figure 3(b) shows the XAS data and the fit at 12 GPa. Figure 3(c) shows the evolution as a function of pressure of the cell parameter of GaP-I as obtained from the Rietveld refinement (circles) and calculated from the bond distances values obtained from the EXAFS analysis.

B. GaP-II

The ADXRD data at 39 GPa show that the GaP-I to GaP-II transition is almost complete although the (111) reflection of the ZB can still be identified at ~7°. The pattern at 39 GPa could be indexed using a *Cmcm* phase and a ZB fraction below 10%. The resulting fit is illustrated in Fig. 4.

The lattice parameter of the ZB structure at 39 GPa is 5.080(4) Å. The refinement of the *Cmcm* phase at 39 GPa gives a=4.679(5) Å, b=4.933(6) Å, and c=4.728(5) Å. The internal coordinates are y(Ga/P)=0.661(7) and y(Ga/P)=0.189(7). The absence of the (111) reflection and the weakness of the (110) at $2\theta \sim 6.3°$ suggest that the structure lack of long-range site order.

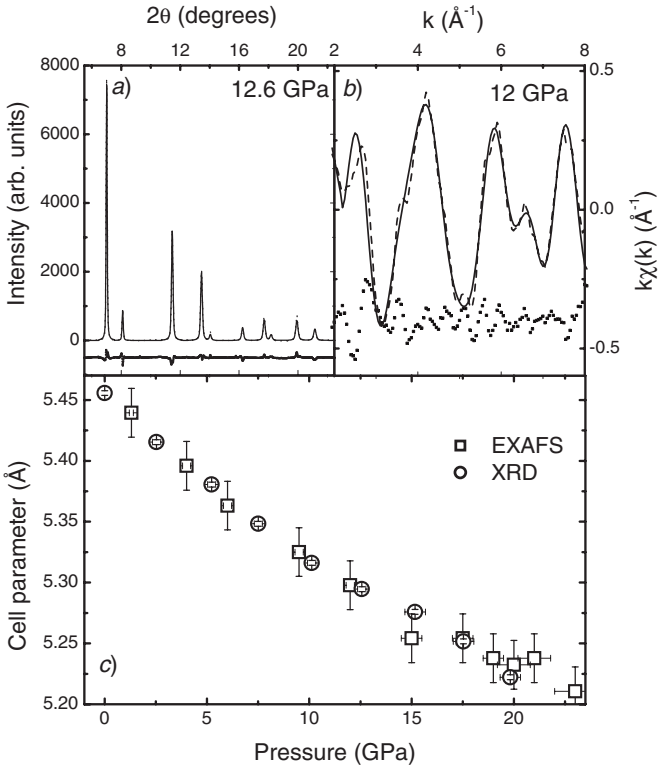

FIG. 3. (a) Rietveld fit of XRD data at 12.6 GPa. (b) XAS data and fit (dashed and continous lines, respectively) at 12 GPa. The bottom dotted line is the residual function. (c) Evolution as a function of pressure of the cell parameters of GaP-I as obtained from Rietveld refinement (circles) and calculated from the bond distances values obtained from the EXAFS analysis (squares).

The analysis of the EXAFS data of GaP in the high pressure region presents an intriguing scenario. In fact, the EXAFS data reported in Ref. 12 could be fitted using a model based on a β-Sn structure for GaP-II that was the only structural model proposed at that time. Nevertheless, in the

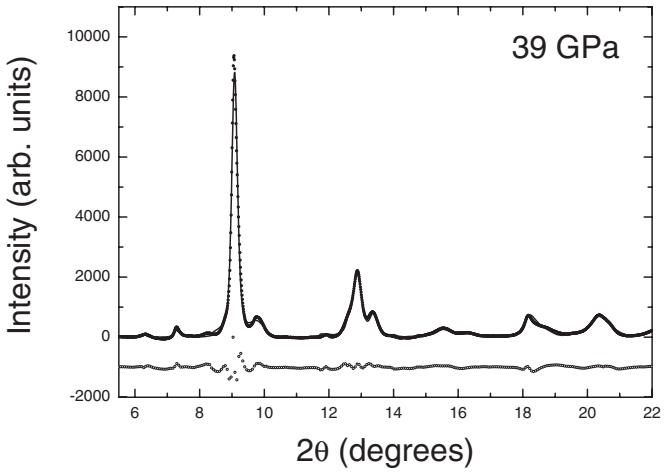

FIG. 4. Rietveld fit (continuous line) of the experimental spectrum (dotted line) at 39 GPa. The bottom curve is the residual function. Two phases are taken into account: The ZB and the *Cmcm*.

TABLE I. Atomic cluster surrounding the Ga atom for GaP in β-Sn and *Cmcm* structures within a distance of 2.7 Å.

	β-Sn		*Cmcm*		
Atom	Dist. (Å)	Deg.	Atom	Dist. (Å)	Deg.
P	2.41	4	P	2.33	1
Ga	2.44	2	P	2.34	2
			P	2.48	2
			P	2.60	1

present work we claim, in agreement with Nelmes *et al.*,[7] that the structure is not β-Sn, but has a *Cmcm* symmetry. We use EXAFS to distinguish β-Sn from *Cmcm*, assuming for the latter a chemically ordered environment. We shall then show from XANES analysis that this assumption is correct.

The local environment of Ga in GaP in an ordered *Cmcm* structure as from the structural parameters reported in this work and in a β-Sn structure as reported by Itié *et al.*[12] are given in Table I.

While in the β-Sn structure the photoabsorber presents two well defined shells of P and Ga, respectively, in the *Cmcm* structure the photoabsorber is surrounded by 6 P atoms at distances between 2.33 Å and 2.60 Å. In Fig. 5(a) we show the calculated $k\chi(k)$ signals relative to the single scattering Ga-P signal at 2.41 Å and to the Ga-Ga signal at 2.44 Å corresponding to the β-Sn local environment. The lower curve represents the sum of the two signals. Figure 5(b) shows the calculated $k\chi(k)$ signals relative to the Ga-P single scattering signals at the four different distances reported in Table I and the lower curve represents the sum. In Fig. 5(c) the two sum curves are compared directly. It is interesting to notice that up to $k \simeq 6$ Å^{-1}, besides a small difference in the overall amplitude, the two calculated curves present a similar main frequency, whereas at higher k the difference between the two curves becomes more important and a fitting over the shown k range should be able to discriminate between the two models. The two compared curves are the sum of calculated $k\chi(k)$ signals where no Debye-Waller factor is included and no fitting is performed.

On the basis of the calculations of the theoretical signals discussed above the fitting of the data at 37.5 GPa was performed using the two structural models. All the results are summarized in Table II. For the β-Sn model two scattering signals were used, corresponding to 4 P atoms at 2.41 Å and 2 Ga atoms at 2.44 Å as nearest neighbors. Leaving the Ga-P and the Ga-Ga distances together with their relative Debye-Waller factors as free parameters (fit β-free on Table II)

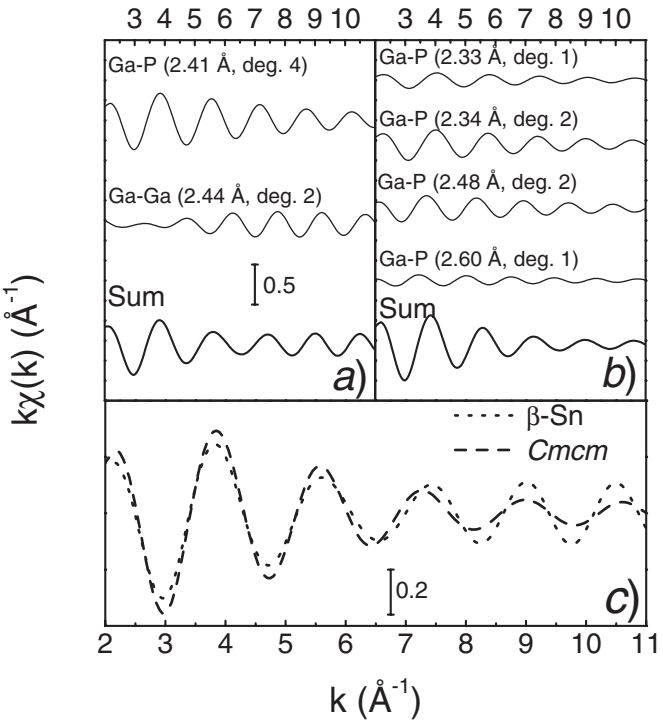

FIG. 5. (a) Calculated $k\chi(k)$ relative to the Ga-P single scattering at 2.41 Å and to the Ga-Ga at 2.44 Å corresponding to the β-Sn local environment. The lower curve represents the sum of the two signals. (b) Calculated $k\chi(k)$ relative to the Ga-P single scattering at the four different distances reported in Table I corresponding to the *Cmcm* local environment. The lower curve represents the sum. (c) Comparison between the two sum curves.

yields Ga-P and Ga-Ga distances not compatible with a β-Sn structure and nonphysical values for the Debye-Waller factors. In order to guarantee a local environment compatible with a β-Sn structure we constrained the two distances Ga-P and Ga-Ga to vary with the same ΔR (fit β-constrained on Table II) and we left the Debye-Waller factors as free parameters. In this case the Ga-Ga signal is overdamped leading to a zero contribution of such a signal in the fitting of the experimental XAFS.

For the *Cmcm* model we have approximated the distribution of the first 6 P atoms as two groups of 3 atoms at two different distances.[23] The structural parameters are reported in Table II.

Figure 6 reports the fit using the *Cmcm* models. Although the residual function (Fig. 6, left panel, bottom curve) contains frequencies associated to higher distances shells and to multiple scattering contributions, the first peak of the Fourier

TABLE II. Structural parameters obtained from the fitting of the experimental data at 39 GPa using the model based on the β-Sn and *Cmcm* structures.

	$R_{\text{Ga-P}}$ (Å)	$\sigma^2_{\text{Ga-P}}$ (Å^2)	N_{P}	$R_{\text{Ga-Ga}}$ (Å)	$\sigma^2_{\text{Ga-Ga}}$ (Å^2)	N_{Ga}	$\mathcal{R}$ factor
β-free	2.35(1)	−0.004(1)	4	2.32(1)	−0.002(1)	2	1.5%
β-constrained	2.38(1)	0.005(1)	4	2.41(1)	0.2(2)	2	2.5%
Cmcm	2.34(1)	0.006(2)	3				1.5%
	2.44(2)	0.007(3)	3				

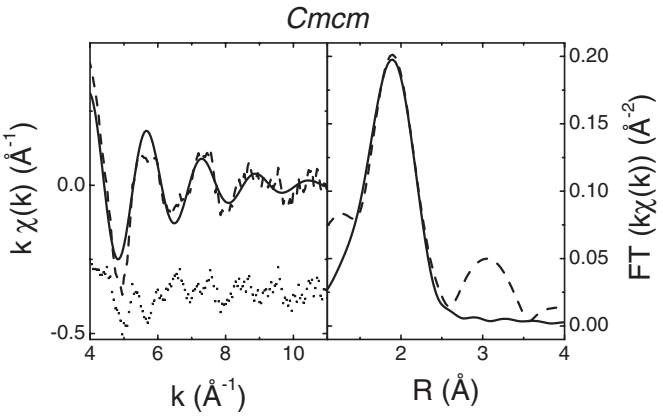

FIG. 6. Left panel: Comparison between the experimental EXAFS spectrum at 37.5 GPa (dashed curve) and the best-fit calculation (solid curve) corresponding to a *Cmcm* environment. The bottom dotted curve shows the residual function. Right panel: Comparison between the modulus of the Fourier transform of the experimental EXAFS spectrum at 37.5 GPa (dashed curve) and the modulus of the Fourier transform of the best-fit calculation (solid curve).

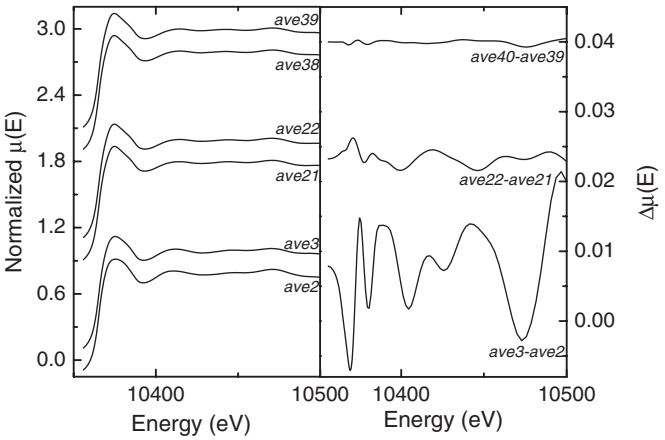

FIG. 7. Left panel: Selected averaged spectra $ave(n)$ and $ave(n-1)$. Right panel: Corresponding differences $ave(n)-ave(n-1)$. The mean value of the point distributions of the differences $ave(n)-ave(n-1)$ approaches zero with the increasing number of clusters over which the averages are calculated.

transform is well reproduced by the best-fit calculation using 2 Ga-P single shells scattering signals. Therefore, the results of the fitting show that the β-Sn structure must be ruled out and GaP crystallizes with a *Cmcm* symmetry above 30 GPa. In order to confirm our results we also performed an additional analysis of the XANES part of the absorption spectra.

V. XANES SIMULATIONS

The low energy part of a XAS spectrum (XANES region) is extremely sensitive to the structural details around the absorbing site such as overall symmetry, distances, and bond angles, and therefore a full retrieval of the geometrical structure within 6–7 Å from the absorbing site can in principle be obtained from the experimental XANES spectra. However, the quantitative analysis of this region presents difficulties mainly related to the theoretical approximation in the treatment of the potential and the need for heavy time consuming algorithms to calculate the absorption cross section in the framework of a full multiple scattering approach. Therefore, we have compared qualitatively our data to *ab initio* simulations obtained by performing full multiple scattering calculations using the FEFF8 package.[20]

A. Method of calculation

We used a self-consistent energy dependent exchange correlation Hedin-Lundqvist potential to simulate the XANES of the high pressure GaP. Self-consistency was obtained by successively calculating the electron density of states, electron density and Fermi level at each stage of the calculation within a cluster centered on the atom of 5.30 Å (56 atoms) and 5.15 Å (34 atoms) of radius for β-Sn and *Cmcm* structures respectively, and then iterating. Full multiple scattering XANES calculations up to a photoelectron wave vector value of $k=6$ Å^{-1} (corresponding to a photoelectron energy of about $E\sim 130$ eV) were carried out for a larger cluster of atoms centered on the photoabsorber of a radius of 6.0 Å (69 atoms) and 6.7 Å (84 atoms) for β-Sn and *Cmcm* structures, respectively. All multiple-scattering paths within these clusters were summed to infinite order. Besides the structural information defining the geometry of the cluster, the only external parameters used as input for the simulations were a constant experimental broadening and an offset in the energy scale. No thermal or static disorder factor was added to the simulations.

We performed simulations for the different observed high pressure phases for GaP: i.e., β-Sn and *Cmcm*. For the β-Sn structure the cluster was built using structural parameters calculated from the Ga-Ga and Ga-P bond distances obtained by Itié *et al.*[12] and assuming that those distances corresponded to a tetragonal cell of space group *I-4m2* with two internal atomic position at (0, 0, 0) and $(0,1/2,1/4)$. The resulting cell parameters were $a=4.663$ Å and $c=2.44$ Å. For the *Cmcm* structure we built ordered as well as disordered clusters. In the former case the composition of each coordination shell was determined by the space group symmetry and by the cell internal site occupation of each atom, as defined by a long range site ordered structure and as obtained by the Rietveld refinement of the ADXRD data. In the latter case, chemically disordered local environments around the absorber atom were approached by randomly mixing the chemical composition of each coordination shell in the chemically ordered clusters. To obtain a simulated XANES spectrum that took into account a random disorder of the structure we used the following strategy. We ran first a FEFF calculation on two chemically disordered clusters: say $d1$ and $d2$. We averaged the two calculated spectra and obtained $ave2$ $(ave2=\langle d1,d2\rangle)$. On a third chemically disordered cluster we simulated a third XANES spectrum: say $d3$. We averaged the three spectra to obtain $ave3=\langle d1,d2,d3\rangle$ and so on. Figure 7 shows (left panel) some selected average spectra $ave(n)$ and $ave(n-1)$ and the corresponding differences $ave(n)-ave(n-1)$ (right panel). After 25 spectra calculated on 25 randomly disordered clusters, the mean value

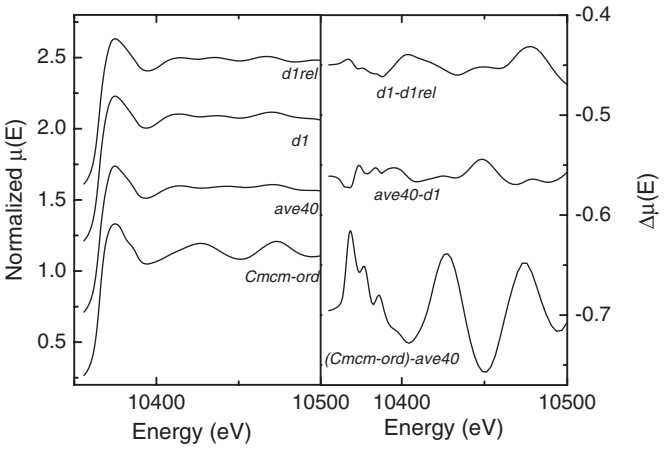

FIG. 8. Left panel: From bottom to top: Simulated spectrum of GaP in the ordered *Cmcm* structure (*Cmcm*-ord). Average of 40 spectra calculated on 40 randomly disordered clusters (*ave40*). Simulated spectrum on a randomly disordered cluster whose difference with the average *ave40* is minimum (*d1*). Spectrum calculated on the same relaxed cluster (*d1rel*) (whole cluster relaxed, $\Delta = \pm 0.04$ Å). Right panel: Difference spectra: From bottom to top: [(*Cmcm-ord*)-*ave40*], *ave40-d1, d1-d1rel.*

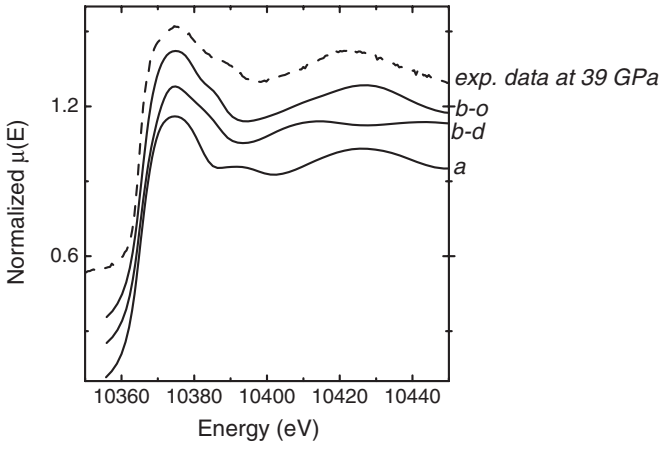

FIG. 9. From bottom to top: Simulated spectra of GaP in β-Sn structure (*a*), in disordered and ordered Cmcm structure (*b-d* and *b-o*), respectively, and the experimental XANES spectrum of GaP at 39 GPa (dashed line).

of the points distribution of $ave(n)-ave(n-1)$ was always less than 10^{-3}.

This way of proceeding assumes rigid Ga-Ga and Ga-P bond lengths. In fact, the different dimensions of the Ga and P atoms as well as the different electronegativities of the Ga-Ga and Ga-P bonds lead inevitably to different Ga-Ga and Ga-P bond lengths (bond relaxation). To take into account and to verify whether and how the effect of the bond relaxation is relevant respect to the chemical mixing, we considered one of the 40 XANES simulations performed on one disordered cluster whose difference with the average of the 40 simulations was minimum. We relaxed the Ga-Ga and Ga-P distances of several amounts from $\Delta = \pm 0.01$ up to $\Delta = \pm 0.04$. For each value of the relaxation parameter we relaxed both (i) the whole cluster and (ii) only the atomic positions at a distance less than 3 Å from the photoasborber. To relax the bond lengths of the requested quantity Δ we scaled the atomic coordinates of each atom such as

$$d_{\text{Ga-Ga}}^{\text{relaxed}} = d_{\text{Ga-Ga}} + \Delta,$$

$$d_{\text{Ga-P}}^{\text{relaxed}} = d_{\text{Ga-P}} - \Delta$$

and such as to conserve the same bond directions as those of the nonrelaxed cluster.

We found that the differences between the simulated spectra on the nonrelaxed and relaxed clusters increase with the relaxation quantity Δ. For the same Δ, relaxation of the whole cluster or only for $r \leqslant 3$ Å from the photoabsorber, gave similar results, indicating that XANES spectra are affected mainly by the positions of the closest atoms. Figure 8 (left panel) shows from bottom to top the simulated spectra of GaP in the ordered *Cmcm* structure (*Cmcm*-ord), the average of 40 spectra calculated on 40 randomly disordered clusters (*ave40*), the simulated spectra on the randomly disordered cluster whose difference with the average *ave40* is minimum (*d1*) and the spectrum calculated on the same relaxed cluster (*d1rel*) (whole cluster relaxed, $\Delta = \pm 0.04$ Å). On the right panel of Fig. 8 we plot the differences between the spectra of the left panel. The difference between the rigid and the relaxed cluster (*d1-d1rel*) is about 2% of the absorption jump, whereas the difference between the chemical disordered and ordered cluster [*(Cmcm-ord)-ave40*] reaches 15% of the absorption jump. Therefore this analysis shows that the relaxation of the bond lengths has a negligible effect respect to the chemical mixing. For this reason, in the following sections we will always refer to the spectrum *ave40* as a model for GaP in the disordered *Cmcm* structure.

B. Results

Figure 9 shows from bottom to top the simulated spectra of GaP in the β-Sn structure (spectrum *a*) and in the disordered and ordered *Cmcm* structures (spectra *b-d* and *b-o*). At energies above 10 400 eV the spectra *a* and *b-o* present similar features, while important variations can be observed just above the absorption edge. In particular the spectrum *a* presents a feature at ~10 390 eV that is not observed in any other simulated spectrum (nor in the experimental one). For the simulated spectra in the *Cmcm* structure, chemically mixing of each shell leads to important variations above 10 390 eV. In fact, the chemical disorder (different atomic species are in the same positions) introduced with the random mixing of each coordination shell almost doubled the main frequency respect to the spectrum *b-o* and heavily reduced the amplitudes of the oscillations. The region just above the absorption edge presents as well differences although the shoulder at the right of the white line is common to the two spectra. The top spectrum of Fig. 9 represents the experimental XANES data at 39 GPa. The agreement with the spectrum *b-o* is striking considering the absence of adjustable parameters in the theory: All the features are well reproduced. The comparison of the data with the simulated spectra excludes a chemical disorder around the Ga atom

(due to the disagreement at energies above 10 390 eV with spectrum *b-d*), and at the same time excludes the occurrence of the β-Sn structure (due to the disagreement just above the absorption edge). This result is consistent with recent XRD diffraction works[7] (including our own), which show chemical disorder on long range. Furthermore, it indicates that whereas chemical order is lost over many lattice cells, or is not detectable by long-range probing techniques (i.e., XRD), GaP on a local atomic scale does conserve a high degree of chemical order.

VI. CONCLUSIONS

In conclusion, we performed combined XRD and XAS measurements on GaP-II up to 39 GPa. XRD data showed that the GaP-II phase has a *Cmcm* symmetry in agreement with previous results. The absence of "difference reflections" indicates a lack of long range chemical order. The EXAFS analysis of data corresponding to GaP-II shows a local environment corresponding to a *Cmcm* structure. Full multiple scattering XANES calculations were used to analyze the local chemical ordering. Indeed, the comparison of the XANES spectra with multiple scattering calculation confirms unequivocally the occurrence of a *Cmcm* symmetry with a high degree of local chemical ordering. This means that, notwithstanding the low ionicity of this compound, this parameter dictates the short range interaction even at high pressures. The local environment of Ga in GaP-II is given by 6 P neighbors and short-range Ga-Ga interactions are not likely to occur in this system at least up to 39 GPa. We have also shown that the relaxation of Ga-P and Ga-Ga distances in the disordered clusters has a negligible effect on the XAS data with respect to that of chemical disorder.

ACKNOWLEDGMENTS

We acknowledge the European Synchrotron Radiation Facility for provision of beamtime through the project HS2103. The experiment at ID30 has been performed during in-house research time. We are also grateful to Sebastien Pasternak for technical support during the experiment at ID24.

*aquilanti@esrf.fr

[1] R. J. Nelmes and M. I. McMahon, J. Synchrotron Radiat. **1**, 69 (1994).
[2] A. Mujica, R. J. Needs, and A. Munõz, Phys. Rev. B **52**, 8881 (1995).
[3] A. Mujica and R. J. Needs, Phys. Rev. B **55**, 9659 (1997).
[4] V. Ozoliņš and A. Zunger, Phys. Rev. Lett. **82**, 767 (1999).
[5] K. Kim, V. Ozoliņš, and A. Zunger, Phys. Rev. B **60**, R8449 (1999).
[6] J. C. Phillips, *Bond and Bands in Semiconductors* (Academic Press, New York and London, 1973).
[7] R. J. Nelmes, M. I. McMahon, and S. A. Belmonte, Phys. Rev. Lett. **79**, 3668 (1997).
[8] M. Mezouar, H. Libotte, S. Députier, T. Le Bihan, and D. Häusermann, Phys. Status Solidi B **211**, 395 (1999).
[9] M. Mezouar, T. Le Bihan, H. Libotte, Y. Le Godec, and D. Häusermann, J. Synchrotron Radiat. **6**, 1115 (1999).
[10] M. Nelmes and A. L. Ruoff, J. Appl. Phys. **53**, 6179 (1982).
[11] J. Z. Hu, D. R. Black, and I. L. Spain, Solid State Commun. **51**, 285 (1984).
[12] J. P. Itié, A. Polian, C. Jauberthie-Carillon, E. Dartyge, A. Fontaine, H. Tolentino, and G. Tourillon, Phys. Rev. B **40**, 9709 (1989).
[13] R. A. Forman, G. J. Piermarini, J. D. Barnett, and S. Block, Science **176**, 284 (1972).
[14] A. P. Hammersley, S. O. Svensson, A. Thompson, H. Graafsma, Å. Kvick, and J. P. Moy, Rev. Sci. Instrum. **66**, 2729 (1995).
[15] S. Pascarelli, O. Mathon, and G. Aquilanti, J. Alloys Compd. **362**, 33 (2004).
[16] H. M. Rietveld, Acta Crystallogr. **22**, 151 (1967).
[17] A. C. Larson and R. B. Von Dreele, Los Alamos National Laboratory Report No. LAUR 86-748, 2004.
[18] E. A. Stern, M. Newville, B. Ravel, Y. Yacoby, and D. Haskel, Physica B **208-209**, 117 (1995).
[19] B. Ravel and M. Newville, Phys. Scr. **T115**, 1007 (2005).
[20] A. L. Ankudinov, B. Ravel, J. J. Rehr, and S. D. Conradson, Phys. Rev. B **58**, 7565 (1998).
[21] B. Ravel, J. Synchrotron Radiat. **8**, 314 (2001).
[22] P. Deaus, U. Voland, and H. A. Schneider, Phys. Status Solidi A **80**, 29 (1983).
[23] Although at this pressure a fraction of the ZB phase may still be present as evidenced by ADXRD, the addition of the ZB contribution does not affect the fitting when the *Cmcm* model is used.